

Effects of Li doping on dielectric properties of $\text{Ag}(\text{Ta}_{0.5}\text{Nb}_{0.5})\text{O}_3$ thick films

Moon-Soon Chae, Jung-Hyuk Koh*

Department of Materials Engineering, Kwangju University, Seoul 139-701, Republic of Korea

Available online 16 October 2012

Abstract

Low loss ferroelectric materials have been extensively investigated for the high frequency device applications. Especially, weak frequency dispersion materials with high dielectric permittivity and low loss tangent have enormous potential for electronic components including filters, and embedded capacitors. $\text{Ag}(\text{Ta}_{0.5}\text{Nb}_{0.5})\text{O}_3$ thick films have been prepared by low temperature sintering aid Li_2CO_3 (0, 1, 3 and 5 wt%). $\text{Ag}(\text{Ta}_{0.5}\text{Nb}_{0.5})\text{O}_3$ thick films were characterized by X-ray diffraction analysis and scanning electron microscopy. The dielectric and ferroelectric properties were also investigated. We observed very weak frequency dispersion of dielectric permittivity at the microwave frequency range.

© 2012 Elsevier Ltd and Techna Group S.r.l. All rights reserved.

Keywords: C. Dielectric properties; $\text{Ag}(\text{Ta}_{0.5}\text{Nb}_{0.5})\text{O}_3$ thick film; Li_2CO_3

1. Introduction

Microwave dielectric materials have been widely used in various applications such as satellite broadcasting, radar antennas and cell phones. High dielectric permittivity over a wide temperature and frequency range has been a very important issue for integrated capacitors. Piezoelectric effect is also an important issue for electronic device applications especially in electromechanical sensors, actuators and transducers [1,2]. In particular, wireless multimedia applications have been considered to enforce a dramatic increase of wireless system capability in the near future. Therefore, the needs for the ferroelectric materials for the microwave applications should be increased.

Silver tantalate niobate, $\text{Ag}(\text{Ta}_x\text{Nb}_{1-x})\text{O}_3$, (hereafter ATN) has been proposed as an alternative dielectric material with good tunability and low dielectric loss property at microwave frequencies [3–7]. ATN ceramics, where $0.4 \leq x \leq 0.6$, show reasonably temperature stable properties and high dielectric permittivity (around 400) at room temperature with weak frequency dispersion up to 100 GHz [8]. $\text{Ag}(\text{Ta}_{0.5}\text{Nb}_{0.5})\text{O}_3$ has a dielectric constant of

~410 at room temperature with a capacitance change, $\Delta C/C$, of less than 8% over the temperature range from -20 to 120°C at 1 MHz [9,10].

Previously, screen printable ATN thick films have been studied because they can reduce fabrication costs. Moreover ATN thick films offer moderate electrical properties compared with thin films. Screen printed thick film can be a flexible, cost-effective device. Thick film devices have relatively low film thickness, resulting in the use of lower biasing voltages compared with those of components prepared in bulk form. However, the sintering temperatures of these films have been over 1150°C [11]. In addition, these high temperatures require the use of palladium electrode instead of silver. Also, lowering the sintering temperature of ATN thick films below 1000°C allows their use with dielectric low-temperature co-fired ceramics (LTCC).

Up to now, Li_2CO_3 is one of the most used additives to lower the sintering temperature of ferroelectric materials. In spite of many investigations, a detailed Li doping mechanism on microstructure properties and dielectric properties have not yet been established.

Therefore, the main objective of this study was to investigate the effect of Li_2CO_3 aid on the low temperature sintering behavior of ATN powders on the alumina

*Corresponding author. Tel.: +82 2 940 5162; fax: +82 2 942 9160.

E-mail address: jhkoh@kw.ac.kr (J.-H. Koh).

(Al₂O₃) substrate by employing the screen printing method. The effect of different lithium conditions on the microstructure of the printed ATN films and their dielectric properties were studied. Also, the high frequency-dependent characteristics of the films were measured.

2. Experiments

A conventional solid-state reaction route was used to synthesize Ag(Ta_{0.5}Nb_{0.5})O₃ powders with Li₂CO₃ as sintering aid with a high purity of 99.9%. The compositions used in this study were as follows: Ag(Ta_{0.5}Nb_{0.5})O₃+*x* wt% Li (where *x*=0, 1, 3, 5, respectively).

Ag₂O, Ta₂O₅, and Nb₂O₅ powders were employed to prepare stoichiometric composition of ATN thick films. After being ball milled for 24 h with ZrO₂ balls and then dried, ATN powders were calcined at 800 °C for 2 h. Then, Li₂CO₃ powders were added to ATN powder. They were ball milled again, dried and calcined. The refined powder size was under 20 μm. After the granulation, MEK (methyl-ethylketone) and alcohol (4:6) in a bottle were mixed with lithium-doped ATN powders. The dispersant (Texaphor 60), bonding agent (PVB binder), and the plasticizer (dibutyl phthalate) were added to this slurry in turn and ball milled. To remove the pores and improve the viscosity, the deaerator was used for 15 min. The Li-doped ATN powders were fabricated by the screen printing method on the alumina substrates and sintered at 950 °C and pure ATN was sintered at 1150 °C for 2 h. Silver interdigital capacitors (hereafter IDC) were patterned through the pattern mask by a manual screen printer. The thickness of lithium-doped ATN thick films was about 10 μm. Interdigital capacitors were composed of five pairs of fingers separated by a 50 mm gap, 100 mm width, and 200 mm length. The crystalline structures were investigated by X-ray diffraction analysis employing Cu-Kα radiation (Rigaku model D/Max-2500 V/PC, Japan). The microstructure was obtained with an SEM (Hitachi S-4300, Japan). The electrical properties of the device were characterized through a Cascade Rel 4500 probe station connected to HP 4284 precision LCR meter, Hp 4194A Impedance analyzer and Keithley 6517A electrometer/high resistance meter. The microwave properties of resonance and reflectance were characterized by a network analyzer Hp 8510C.

3. Results and discussions

Fig. 1 shows the XRD diffraction patterns of ATN–*x* wt% Li₂CO₃ (0 ≤ *x* ≤ 5) thick films (10 μm) on the alumina substrate sintered at 1150 and 950 °C. The Ag(Ta_{0.5}Nb_{0.5})O₃ films have perovskite structure with weak pyrochlore phases. Peaks from the alumina substrate were also visible in the diffraction patterns. With an increase in the amount of Li₂CO₃ added, the lattice constant initially increases to a maximum at *x*=1 wt%, and then decreases again to a minimum at *x*=5 wt%.

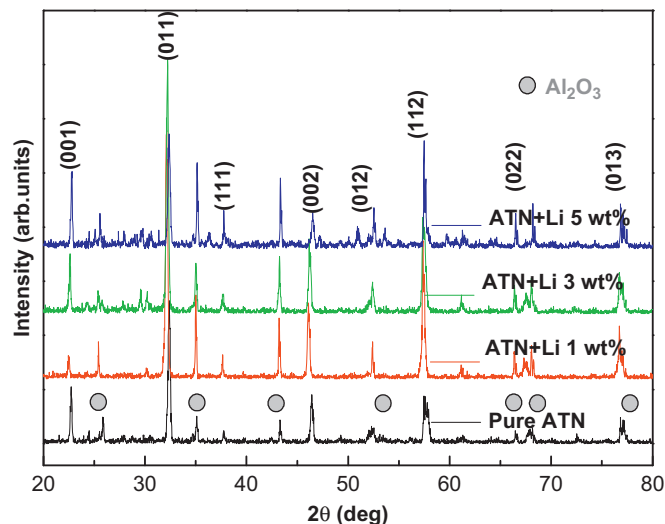


Fig. 1. X-ray diffraction (XRD) patterns of *x* wt% Li-doped ATN thick films.

Table 1

Lattice parameters *c* and *a* of the ATN with addition of *x* wt% Li₂CO₃.

Li ₂ CO ₃ content (wt%)	Lattice parameters (Å)	
	<i>c</i>	<i>a</i>
Pure ATN	3.915	3.941
ATN+Li 1%	3.922	3.948
ATN+Li 3%	3.919	3.945
ATN+Li 5%	3.913	3.939

The lattice parameter was calculated by Nelson–Riley extrapolation function with the least mean square method. The equation can be expressed as follows [12]:

$$\frac{C_{\cos\theta} - C_0}{C_0} = A \cos^2\theta \left(\frac{1}{\sin\theta} + \frac{1}{\theta} \right), \quad (1)$$

where $C_{\cos\theta}$ is the interplane distance calculated from the apparent Bragg peak position at 2θ and A is a fitting coefficient. The calculated lattice parameters *c* and *a* of ceramics are 3.922–3.913 Å and 3.939–3.948 Å, respectively. The variations of lattice parameters as a function of the lithium condition of ATN thick films are shown in Table 1.

In an ideal perovskite ABO₃ of Ag(Ta_{0.5}Nb_{0.5})O₃ structure, the ionic radii of Ag, Li, Ta, Nb and O are summarized as follows: A-site (12 coordinate): Ag¹⁺=1.22 Å; B-site (6 coordinate): Nb⁵⁺=0.64 Å and Ta⁵⁺=0.64 Å, Li¹⁺=0.76 Å; O²⁻=1.40 Å. Accordingly, the Li¹⁺ would occupy the B-site with Nb⁵⁺ and Ta⁵⁺ [13]. Therefore, charges of lattice constant are determined by the cation substitution.

Fig. 2 shows the SEM micrographs of pure ATN and Li-doped ATN thick films sintered at 1150 °C and 950 °C, respectively. All the sintered specimens showed a somewhat

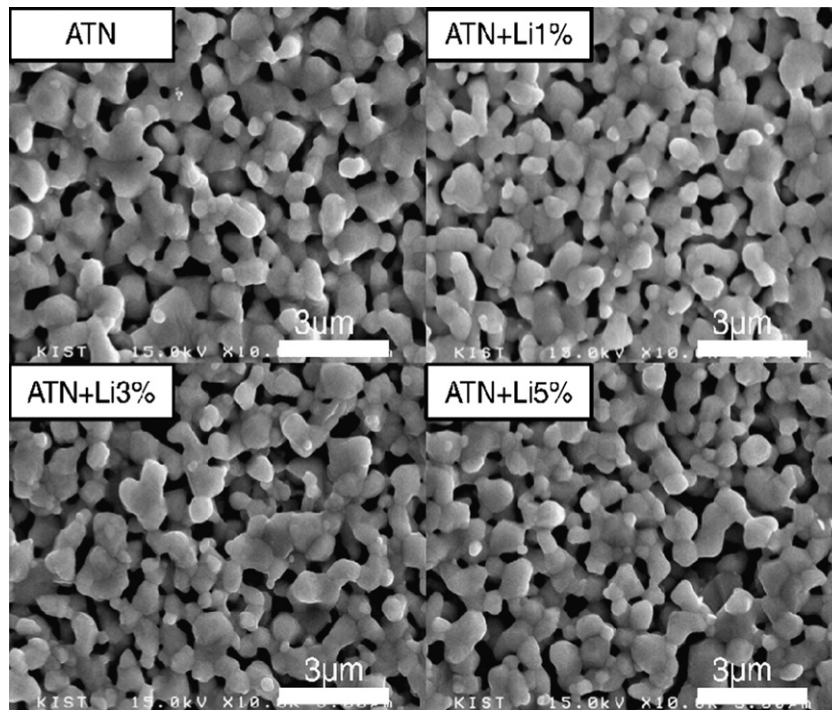
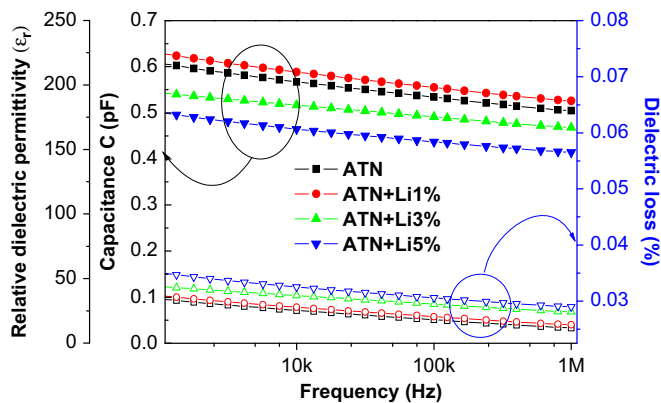
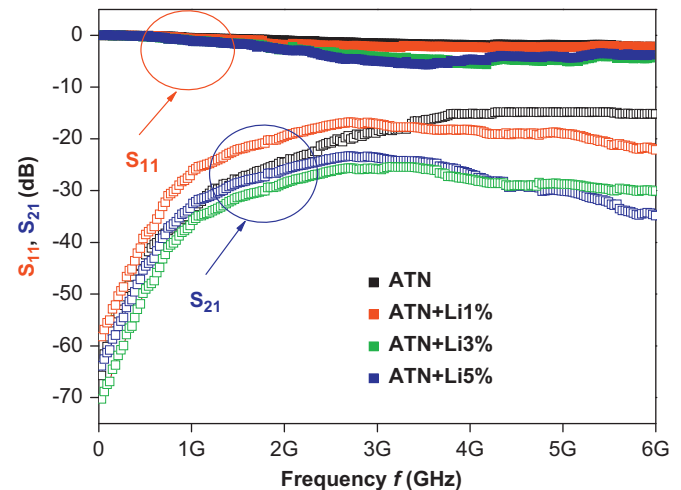


Fig. 2. SEM images of sintered Li-doped ATN thick films.

Fig. 3. Frequency dependencies of capacitance and dissipation factor $\tan\delta$ from 1 kHz to 1 MHz range.

porous microstructure. The grain sizes of Li-doped ATN specimens are almost the same. In addition, the density values were 67, 69, 66, and 65 vol% for ATN, 1 wt% Li-doped ATN, 3 wt% Li doped ATN, and 5 wt% Li doped ATN thick films, respectively. Obviously, the addition of a small amount of lithium results in significant improvement in sinterability of ceramics [14].

Fig. 3 illustrates the frequency dependent capacitance and loss tangent of Li-doped ATN thick films (10 μm) IDC in the frequency range from 1 kHz to 1 MHz. With increasing of Li dopant up to 1 wt% in the ATN thick films, the capacitance increased from 0.6 pF to 0.63 pF. Then, as the Li dopant increased to 5 wt%, the capacitance rapidly decreased to 0.5 pF. Relative dielectric permittivity was simulated by considering the capacitor's geometry including finger length, gap, and film thickness. The simulated relative

Fig. 4. Microwave scattering parameters of S_{11} and S_{21} properties of Li-doped ATN thick films interdigital capacitors on the alumina substrates.

dielectric permittivity was placed between 214 at 10 kHz and 182 at 1 MHz. The relative dielectric permittivities of thick films were simulated through the conformal mapping analysis from the measured capacitance. Since ATN compositions are well-known as the microwave materials [4], the dielectric loss has slightly decreased from 0.035% to 0.026%. ATN thick films have low loss tangent properties with negligible change at all frequencies. Thus, we believe low temperature sintered Li doped ATN thick films (1 wt% Li-doped ATN thick films) maintain the microwave properties of pure ATN ceramics.

Fig. 4 shows the microwave properties of Li-doped ATN thick film (10 μm) interdigital capacitors measured from

0 to 6 GHz at room temperature. As shown in the figure, the reflection coefficients (S_{11}) of 0, 1, 3 and 5 wt% Li-doped ATN thick films were reduced slowly with increasing frequency. The S_{21} of Li-doped ATN thick films revealed the capacitive properties up to 3 GHz range, and the resonance frequency of interdigital capacitors with inductive properties was present from 3 GHz. This resonance probably came from the inserted parasitic inductance. The parasitic inductance mainly comes from the long finger length of 200 μm in the interdigital capacitor. S_{21} parameter also had a value lower than -50 dB at lower frequency of up to 100 MHz. It shows the open-circuit capacitive properties at low frequency range.

4. Conclusion

Li-doped ATN thick film interdigital capacitors were fabricated on the alumina substrates. The sintering temperature of ATN thick film was 950 °C under Li doping. From the X-ray diffraction analysis, Li-doped ATN thick films showed the perovskite structure. The loss tangent of Li doped ATN thick film was 0.026% at 1 MHz range with very weak frequency dispersion. Microwave transmission (S_{21}) and reflectance (S_{11}) properties of interdigital capacitors were also measured. The parameters S_{21} increased from -70 dB to -20 dB and S_{11} decreased from 0 dB to -5 dB.

Acknowledgments

This research was funded by the Ministry of Education, Science and Technology (Grant No. 2010-0011536) and the National Research Foundation of Korea (NRF) grant (MEST) (No. 2011-0029625).

References

- [1] S.G. Lu, X.H. Zhu, C.L. Max, K.H. Woog, H.L.W. Chan, C.L. Choy, High tenability in compositionally graded epitaxial

- barium strontium titanate thin films by pulsed-laser deposition, *Applied Physics Letters* 82 (2003) 2877–2879.
- [2] S.G. Lee, S.E. Moon, H.C. Ryu, M.H. Kwak, Y.T. Kim, Microwave properties of compositionally graded (Ba,Sr)TiO₃ thin films according to the direction of the composition gradient for tunable microwave applications, *Applied Physics Letters* 82 (2003) 2133–2135.
- [3] F. Zimmermann, W. Menesklou, E. Ivers-Tiffée, Investigation of Ag(Ta,Nb)O₃ as tunable microwave dielectric, *Journal of the European Ceramic Society* 24 (2004) 1811–1814.
- [4] J.H. Koh, B.M. Moon, A. Grishin, Dielectric properties and Schottky barriers in silver tantalate–niobate thin film capacitors, *Journal of Integrated Ferroelectrics* 39 (2001) 1361–1368.
- [5] M.H. Fracombe, B. Lewis, Structure and electrical properties of silver niobate and silver tantalate, *Acta Crystallographica* 11 (1958) 175–178.
- [6] A. Kanla, AgNb_{1-x}Ta_xO₃ solid solutions—dielectric properties and phase transitions, *Phase Transitions* 3 (1983) 131–140.
- [7] M. Pawelczyk, Phase transitions in AgTa_xNb_{1-x}O₃ solid, *Phase Transitions* 8 (1987) 273–292.
- [8] A.A. Volkov, B.P. Gorshunov, G. Komandin, W. Fortin, G.E. Kugel, A. Kania, J. Grigas, High-frequency dielectric spectra of AgTaO₃–AgNbO₃ mixed ceramics, *Journal of Physics: Condensed Matter* 7 (1995) 785–793.
- [9] J. Petzelt, S. Kamba, E. Buixaderas, V. Bovtun, Z. Zikmund, A. Kania, V. Koukal, J. Pokorny, J. Polivka, V. Pashkov, G. Komandin, A. Volkov, Infrared and microwave dielectric response of the disordered antiferroelectric Ag(Ta,Nb)O₃ system, *Ferroelectrics* 223 (1999) 235–246.
- [10] M. Valant, D. Suvorov, New high permittivity AgNb_{1-x}Ta_xO₃ microwave ceramics: part 2, dielectric characteristics, *Journal of the American Ceramic Society* 82 (1999) 88–93.
- [11] K.T. Lee, J.H. Koh, The electric and dielectric properties of Ag(Ta_{0.5}Nb_{0.5})O₃ and Ag(Ta_{0.8}Nb_{0.2})O₃ thick films, *Current Applied Physics* 11 (2011) S56–S59.
- [12] J.H. Koh, S.J. Jeong, M.S. Ha, S.J. Song, Aging of piezoelectric properties in Pb(MgNb)O₃–Pb(ZrTi)O₃ multilayer ceramic actuators, *Journal of Applied Physics* 96 (2004) 544–548.
- [13] R.D. Shannon, Revised effective ionic radii and systematic studies of interatomic distances in halides and chalcogenides, *Acta Crystallographica A* A32 (1976) 751–767.
- [14] D. Lin, K.W. Kwok, H.L.W. Chan, Piezoelectric and ferroelectric properties of K_xNa_{1-x}NbO₃ lead-free ceramics with MnO₂ and CuO doping, *Journal of Alloys and Compounds* 461 (2008) 273–278.